Obtaining spatial information from an extremely unresolved source

Grover A. Swartzlander, Jr.

Chester F. Carlson Center for Imaging Science and the Department of Physics, Rochester Institute of Technology, 54 Lomb Memorial Drive, Rochester, New York 14623, USA (gaspci@rit.edu)

Received September 20, 2011; revised October 29, 2011; accepted November 2, 2011; posted November 2, 2011 (Doc. ID 154696); published December 9, 2011

A means to extract spatial information from an extremely unresolved source of light using a single element detector is demonstrated by use of an optical vortex coronagraph. Applications may range from astronomy to microscopy. For example, the centroid and angular extent of an unresolved collection of incoherent point sources is revealed. © 2011 Optical Society of America

OCIS codes: 110.2990, 110.2970, 080.4865, 100.6640.

An object or collection of objects may be said to be unresolvable in a given optical system if the apparent image is indistinguishable from a single point source of light. Although resolution can be improved by use of short focal length, large aperture elements, this approach is not always cost effective or practical. For example, a conventional imaging system may be unnecessary if the desired information is simply the position and extent of a system of a few emitters, as may be the case with fluorescent, nano-optic, astronomical, or microsatellite systems. Herein is described a means of using an optical vortex coronagraph [1,2] to extract the centroid and extent of an extremely unresolved object. An advantage of this approach is that large f-number optics may be used. Such elements are less prone to aberrations, inexpensive, and lightweight in comparison to small f-number optics. What is more, a single detector element may be used in the optical vortex coronagraph (OVC) system, rather than an imaging array. The technique requires subresolution pointing stability of the optical system and absolute power measurements.

A spatial filtering scheme using an optical vortex "lens" was first proposed as a two dimensional Hilbert filter [3]. This approach was successfully used in microscopy as an alternative to conventional phase contrast microscopy techniques [4]. Vortex coronagraphs were initially devised as a high contrast imaging instrument to observed exoplanets [1,2,5]. Astronomers have recently succeeded in observing exoplanets with an OVC [6].

An OVC performs an important operation: it completely filters out light from a point source when the optical axis and the source coincide. Hence, the OVC has the capacity to strip away the point source (or zero spatial frequency) information to reveal information about the structure of the source. An optical vortex lens (or "spiral phase plate") is placed in the focal plane of the objective lens, as illustrated in Fig. 1. The required transmission function of the vortex element is $t = \exp(im\theta')$, where θ' is the azimuth in the $x'y'$ plane, and m is the so-called topological charge of the vortex. The OVC requires a nonzero even value of m. As shown below, it is sufficient to consider the case $m = 2$ to determine the centroid and radial variance of the distribution. Larger values of m may be used to obtain higher order moments of the distribution. Paraxial, subresolution ray angles are assumed below: $\alpha \ll \lambda/2R$, where λ is the wavelength of light, and R is the radius of the objective lens.

Owing to symmetry of the OVC we describe the optical fields in terms of separable functions and circular coordinates. The field of the source distribution is expressed as a Fourier series of circularly harmonic vortex modes of index, l:

$$f(r_0, \theta_0) = \sum_{l=-\infty}^{\infty} B_l(r_0) \exp(il\theta_0), \tag{1}$$

where $B_l(r_0) = (1/2\pi) \int_0^{2\pi} f(r_0, \theta_0) \exp(-il\theta_0) \mathrm{d}\theta_0$. When the distance between the object and the imaging system is large ($z \gg \pi a^2/\lambda$), as depicted in Fig. 2, the field at the objective lens may be described by Fraunhofer diffraction.

Owing to the principle of linear superposition each mode in Eq. (1) undergoes a Fourier transform upon reaching the objective:

$$E_l(r, \theta) = (2\pi/\lambda z)(-i)^l \exp(il\theta) HT_l\{B_l(r_0)\}, \tag{2}$$

where $HT_l\{B_l(r_0)\} = \int_0^{\infty} B_l(r_0) J_l(k_r r_0) \mathrm{d}r_0$ is an lth order Hankel transform, $k_r = 2\pi r/\lambda z$ is the radial component of the transverse wave vector, and $J_l(k_r r_0)$ is the lth order Bessel function of the first kind. The maximum value of the argument provides a subresolution criterion:

$$\gamma = 2\pi Ra/\lambda z \ll 1. \tag{3}$$

Replacing the Bessel functions with the expression

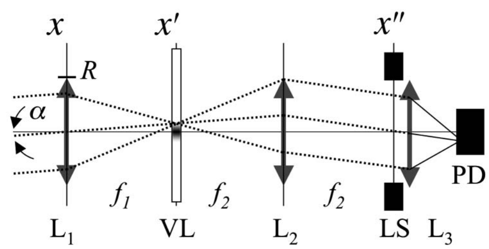

Fig. 1. Optical vortex coronagraph with objective lens of radius R (L_1), vortex lens (VL), collimating lens (L_2), Lyot stop of radius R_{Lyot} (LS), condenser lens (L_3), and photo detector (PD). Ray trace for incident plane wave (dashed lines).

0146-9592/11/244731-03$15.00/0

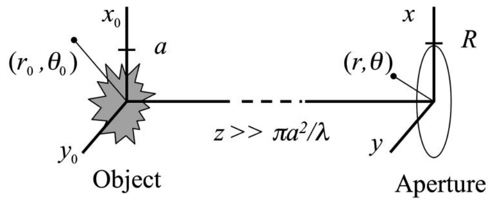

Fig. 2. Light from an object of extent a is transmitted to the circular aperture of an objective lens of radius R.

$$J_l(k_r r_0) = \sigma(l)\left(\frac{k_r r_0}{2}\right)^L \sum_{n=0}^{\infty}\left(-\left(\frac{k_r r_0}{2}\right)^2\right)^n / (n!(n+L)!), \tag{4}$$

where $L = |l|$ and $\sigma(l) = 1$ if $l \geq 0$, otherwise $\sigma(l) = (-1)^l$ [7], the transmitted field at the circular pupil function of the objective may therefore be written, for $r \leq R$:

$$E(r, \theta) = \sum_{l=-\infty}^{\infty}\sum_{n=0}^{\infty} C_{l,n}(r/R)^p \exp(il\theta), \tag{5}$$

where $p = L + 2n$, and

$$C_{l,n} = \frac{(-1)^n(-i)^l 2\pi}{n!(n+L)!}\frac{(\pi R/\lambda z)^p}{\lambda z}\int_0^a B_l(r_0) r_0^{p+1} \mathrm{d}r_0. \tag{6}$$

The field in the back focal plane of the objective lens is given by the Fourier transform of Eq. (5). Transmission through the vortex lens gives for each mode of index l, n:

$$g_{l,n}^{(m)}(r', \theta') = 2\pi(-i)^l C_{l,n} e^{i(m+l)\theta'}\int_0^R \left(\frac{r}{R}\right)^{p+1} J_l(k_r' r)\mathrm{d}r, \tag{7}$$

where $k_r' = 2\pi r'/\lambda f_1$. The beam undergoes another Fourier transform upon propagating to the Lyot stop, where the modes may be expressed $G_{l,n}^{(m)}(r'', \theta'') = A_{l,n}^{(m)}(\theta'') I_{l,n}^{(m)}(r'')$:

$$A_{l,n}^{(m)}(\theta'') = 4\pi^2(-i)^{2l+m} C_{l,n} e^{i(l+m)\theta''}, \tag{8a}$$

$$I_{l,n}^{(m)}(r'') = \int_0^{\infty}\int_0^R ((r/R)^p J_l(k_r' r) r \mathrm{d}r) J_{l+m}(k_r'' r') r' \mathrm{d}r', \tag{8b}$$

where $k_r'' = 2\pi r''/\lambda f_2$ and Eq. (8b) reduces to Weber-Schafheitlin integrals having closed form polynomial solutions. In some cases Eq. (8b) vanishes within the reimaged pupil where $r'' < R'' = f_2 R/f_1$, resulting in a "ring of fire" that is completely blocked by a Lyot stop of radius $R_{\mathrm{Lyot}} \leq R''$. As demonstrated below, modes that are transmitted through the Lyot stop will reveal information about the unresolved light source. We assume $R_{\mathrm{Lyot}} = R''$.

From both a theoretical and experimental point of view, it is instructive to consider a system of radiating point sources, as depicted in Fig. 3. These could be fluorescing nanoparticles, a distant star system, or orbiting space debris. A single source may be represented in circular coordinates by a delta function at the point (a_j, θ_j), having a phase, Φ_j: $f(r_0, \theta_0) = a_j^{-1}\delta(r_0 - a_j)\delta(\theta_0 - \theta_j)\exp(i\Phi_j)$.

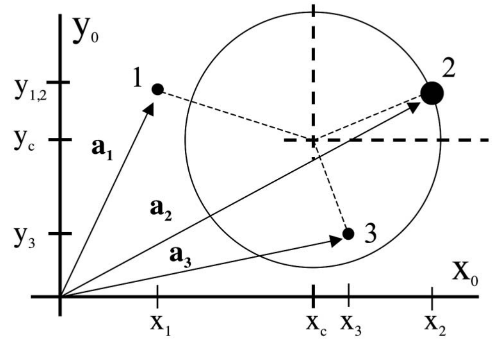

Fig. 3. Distribution of point sources with centroid at the origin of the dashed axes. Coronagraph optical axis at origin of solid axes. Circle depicts the radial deviation of the distribution.

Consider first a single point source. The mode $(l, n) = (0, 0)$ represents the *apparent* on-axis point source component of the source (even if the source is neither on-axis, nor a point source). This is the dominant mode that we wish to eliminate with the OVC so as to reveal weaker modes. For the region within the Lyot stop, $r'' < R_{\mathrm{Lyot}}$, it may be shown that

$$G_{0,0}^{(m)}(r'', \theta'') = G_0 e^{i\Phi_j}\begin{cases} 1, & m = 0 \\ 0, & m = \pm 2, \pm 4, \ldots \end{cases} \tag{9}$$

where $G_0 = \lambda f_1^2/z$. The $m = 0$ case corresponds to the reimaged objective aperture. To establish the underlying method, the $m = 2$ case is treated below.

The mode $(l, n) = (1, 0)$ is also zero valued within the Lyot stop. The lowest order transmitted mode corresponds to $(l, n) = (-1, 0)$:

$$G_{-1,0}^{(2)}(r'', \theta'') = -i(G_0/2)(r''/R'')\gamma_j e^{i(\theta_j + \Phi_j + \theta'')}, \tag{10}$$

where $\gamma_j = 2\pi R|a_j|/\lambda z$. The next highest order mode that transmits through the Lyot stop is found to be

$$G_{0,1}^{(2)}(r'', \theta'') = -(G_0/8)(r''/R'')^2\gamma_j^2 e^{i(\Phi_j + 2\theta'')}. \tag{11}$$

The transmitted power $P^{(m)}$ is given by the integrated intensity of light through the Lyot stop:

$$P^{(2)} = \int_0^{2\pi}\int_0^{R_{\mathrm{Lyot}}} |G_{-1,0}^{(2)} + G_{0,1}^{(2)} + \ldots|^2 r'' \mathrm{d}r'' \mathrm{d}\theta''. \tag{12}$$

Comparing this to the transmitted power with the vortex lens removed,

$$P^{(0)} = \int_0^{2\pi}\int_0^{R_{\mathrm{Lyot}}} |G_0|^2 r'' \mathrm{d}r'' \mathrm{d}\theta'', \tag{13}$$

one obtains the ratio, to leading order, of two easily measured values:

$$\eta^{(2)} = P^{(2)}/P^{(0)} = (1/8)\gamma_j^2 + O(\gamma_j^4). \quad (14)$$

For a distribution of N point sources, the power transmitted through the Lyot stop will depend on the mutual coherence of the sources. For interfering coherent sources, it may be necessary to include the contributions of Eq. (11) because the lower order term may cancel owing to interference. However, for incoherent sources, Eq. (11) is negligible. The relative transmission may then be written

$$\eta^{(2)}(x_0, y_0) = (1/8)\sum_{j=1}^{N} \gamma_j^2 \varepsilon_j, \quad (15)$$

where ε_j is the normalized brightness of the jth source with $\sum_{j=1}^{N} \varepsilon_j = 1$, and the origin (x_0, y_0) mark the position of optical axis of the OVC [see Fig. 3]. The value of Eq. (15) is a minimum at the centroid of the distribution, as illustrated by the curve $P^{(2)}$ at $\alpha = 0$ in Fig. 4. What is more, when (x_0, y_0) is positioned at the centroid of the distribution, Eq. (15) is equal to 1/8th the radial variance of the distribution. The centroid of an unresolved distribution of sources may be found by angularly scanning the OVC to locate the minimum value of $\eta^{(2)}$, at which point the measured power is proportional to the variance of the distribution. The value $P^{(0)}$ is expected to remain constant over small scan angles, and thus it is sufficient to locate the minimum value of $P^{(2)}$. This technique may be useful for targeting and tracking unresolved objects, honing a guidestar, or determining distances between distributions.

Conventional imaging of a point source produces an intensity peak that varies for small angles as $1 - (1/8)(\alpha/\alpha_d)^2$ where $\alpha = a_1/z$ and $\alpha_d = 1.22\lambda/2R$ (see "Point Image" in Fig. 4). Similarly, the angular variation for the $m = 2$ OVC may be written as $(1/8)(\alpha/\alpha_2)^2 + \mathrm{const}$ where $\alpha_2 = \lambda/2\pi R$. The smaller value $\alpha_2 = \alpha_d/3.83$ provides the OVC with a potential advantage for locating the centroid, as discussed below. Once the signal is determined at the centroid, the OVC provides a simple means of determining the variance of the distribution. For example, if we measure $P^{(2)} = 0 \pm \delta P^{(2)}$, we say that the source is a single point source to within an error of $\delta\alpha = (\lambda/2\pi R)\sqrt{8\delta P^{(2)}/P^{(0)}}$. If $\delta P^{(2)}/P^{(0)} = 10^{-6}$, then $\delta\alpha \approx 10^{-3}\alpha_d$.

A comparison of measured signals for a conventional imaging system and an $m = 2$ OVC is represented by computer-generated data dominated by additive noise in Fig. 4. The plots suggest that noisy measurements across a subresolution range may be used, along with a least squares fit assessment, to extract the values of α_2 and $P^{(2)}$ without large errors (0.85% and 9%, respectively). Repeated measurements would allow greater precision. Note that the width of the conventional image is not well-sampled, and therefore the error (11%) is significantly higher than the OVC case.

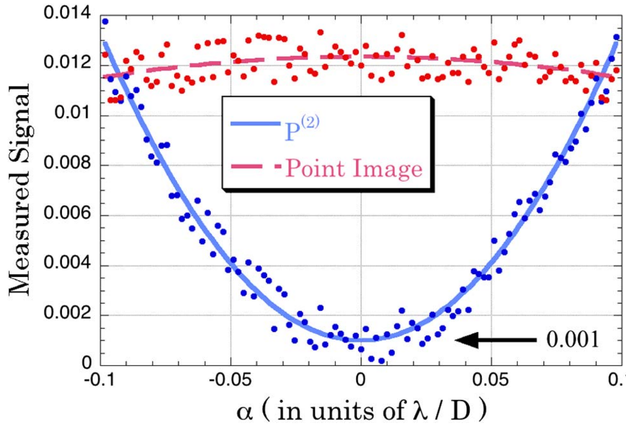

Fig. 4. (Color online) Computer-generated signals with additive noise for an OVC ($m = 2$) and a conventional imaging system ($m = 0$) having respective widths $0.318\lambda/D$ and $1.22\lambda/D$ (λ wavelength, D objective aperture diameter). The offset OVC minimum indicates that the radiating object has a nonzero angular extent.

In summary a means to extract moments of an unresolved distribution of point sources has been established. In particular, the radial variance of the distribution is determined by simply measuring the transmitted power through an $m = 2$ optical vortex coronagraph at the centroid of the distribution. The position of the centroid corresponds to the angular position where the transmitted power has a minimum value. The theoretical approach presented here can be generalized for arbitrary distributions of light and for other even values of topological charge. Higher charges are expected to reveal higher order moments of the light distribution. Experiments using a high quality vortex lens produced with microlithography techniques are underway.

The author is grateful to Mark Dennis, Univ. Bristol, and Jiaxuan Han, Rochester Institute of Technology, for discussion regarding calculations involving higher values of the topological charge.

References

1. D. Mawet, P. Riaud, O. Absil, and J. Surdej, Astrophys. J. **633**, 1191 (2005).
2. G. Foo, D. M. Palacios, and G. A. Swartzlander Jr., Opt. Lett. **30**, 3308 (2005).
3. S. N. Khonina, V. V. Kotlyar, M. V. Shinkaryev, V. A. Soifer, and G. V. Uspleniev, J. Mod. Opt. **39**, 1147 (1992).
4. S. Furhapter, A. Jesacher, S. Bernet, and M. Ritsch-Marte, Opt. Express **13**, 689 (2005).
5. G. A. Swartzlander, Jr., Opt. Lett. **26**, 497 (2001).
6. E. Serabyn, D. Mawet, and R. Burruss, Nature **464**, 1018 (2010).
7. M. Abramowitz, and I. A. Stegun, *Handbook of Mathematical Functions*, 9th ed. (Dover, 1972).